Open Archive TOULOUSE Archive Ouverte (OATAO)

OATAO is an open access repository that collects the work of Toulouse researchers and makes it freely available over the web where possible.

Any correspondance concerning this service should be sent to the repository administrator: staff-oatao@inp-toulouse.fr.

Purification of biomimetic apatite-based hybrid colloids intended for biomedical applications: A dialysis study

Ahmed Al-kattan [a,b], Pascal Dufour [b], Christophe Drouet [a,*]

[a] CIRIMAT Carnot Institute–Phosphates, Pharmacotechnics, Biomaterials, University of Toulouse, CNRS/INPT/UPS, ENSIACET, 4 allée Emile Monso, 31030 Toulouse cedex 4, France
[b] CIRIMAT Carnot Institute, University of Toulouse, CNRS/INPT/UPS, LCMIE, Université Paul Sabatier, 118 route de Narbonne, Bât. 2R1, 31062 Toulouse cedex 9, France

ABSTRACT

The field of nanobiotechnology has lately attracted much attention both from therapeutic and diagnosis viewpoints. Of particular relevance is the development of colloidal formulations of biocompatible nanoparticles capable of interacting with selected cells or tissues. In this context, the purification of such nanoparticle suspensions appears as a critical step as residues of unreacted species may jeopardize biological and medical outcomes, and sample purity is thus increasingly taken into account by regulatory committees. In the present work, we have investigated from a physico-chemical point of view the purification by dialysis of recently developed hybrid colloids based on biomimetic nanocrystalline apatites intended for interacting with cells. Both Eu-doped (2 mol.% relative to Ca) and Eu-free suspensions were studied. The follow-up of the dialysis process was carried out by way of FTIR, TEM, XRD, pH and conductivity measurements. Mathematical modelling of conductivity data was reported. The effects of a change in temperature (25 and 45 °C), dialysis medium, and starting colloid composition were evaluated and discussed. We show that the dialysis method is a well-adapted and cheap technique to purify such mineral–organic hybrid suspensions in view of biomedical applications, and we point out some of the characterization techniques that may prove helpful for following the evolution of the purification process with time.

Keywords:
Colloid
Purification
Dialysis
Biomimetic apatite
Nanomedicine

1. Introduction

During the last decade a lot of efforts have been dedicated to develop innovative nanosystems [1–5], often formulated as colloids, capable of interacting specifically with cells and tissues. A particularly developed domain of investigation involves cancer cells targeting. The idea is here to improve the efficacy of cancer treatments while significantly reducing side effects, and to facilitate early diagnosis therefore limiting cancer-related mortality. Indeed, according to the International Agency for Research on Cancer (CIRC), 24 million people are currently affected by cancer worldwide [6]. In its 2008 World cancer report, this Agency estimated that the number of patients concerned by this disease, originating from the anarchical proliferation of some cells, had doubled between the years 1970 and 2000.

In the field of cancer diagnosis in particular, medically oriented detection techniques based on luminescent nanoprobes capable of interacting with cells have particularly raised interest in the view of tumour detection. Among the nanoprobes commonly considered for medical imaging are organic dyes such as DAPI or green fluorescence protein [7] or semiconductor quantum dots [8–10]. However, these systems appear to be either toxic [11,12] or non-suitable for the analysis of biological tissues over extended periods of time due to photobleaching or flickering effects [13,14]. Taking account of these above observations, alternative nanosystems have been investigated, such as lanthanide-doped inorganic nanoparticles characterized by narrow emission bandwidths, high photochemical stability and long fluorescence lifetime (up to several milliseconds). Also, as for quantum dots, different colours are available by varying the luminescent centre used, e.g. Tb, Eu, Dy [15–18]. In this view, we have successfully synthesised recently by soft chemistry, stable luminescent colloidal systems based on biomimetic nanocrystalline apatite analogous to bone mineral [19], $Ca_{10-x}(PO_4)_{6-x}(HPO_4)_x(OH)_{2-x}$ $(0 \leq x \leq 2)$, doped with a few atomic % of rare-earth element [20].

In our previous work [20], the synthesis and physico-chemical characteristics of such colloids (size, morphology, composition and luminescence properties) were investigated and perspectives in terms of biological evaluations were commented. The synthesis protocol used for preparing such colloidal apatite nanoparticles involves the use of ionic salts, some of which being used in excess,

---

and a purification process is then necessary for eliminating unreacted salts.

More generally, purification may appear as one of the limiting steps of development of potentially promising nanoscale systems and should not be under-estimated. In fact, it should probably be considered early in the process of developing innovative systems, as remaining traces of unreacted reagents, catalysts or organic solvents may lead to biased biological results or the impossibility to comply with regulatory aspects.

Two categories of procedures are often encountered (e.g. in pharmaceutical or agro-alimentary developments) for purifying suspensions.

A first approach consists in preliminarily separating the solid particles from the liquid medium by way of filtration (e.g. vacuum filtration or syringe filtering) or fast-drying methods (e.g. in fluidized-bed) and subsequently washing the obtained powder or gel with an appropriate pure solvent such as deionised water. However, this procedure is not straightforward as it requires both a separation and a washing step. Also, the filtration may appear in itself difficult in the case of nano-sized particles as they can often pass through the pores of filters, resulting in inefficient filtration, while smaller pores can rapidly be obstructed by accumulated particles leading to extremely low filtration yields. Finally, the possibility to re-suspend the particles at the end of the process often proves to be problematic due to some irreversible agglomeration of adjacent particles during the separation step.

The second approach aims at retaining the nanoparticles in a wet state throughout the whole cleansing process in order to avoid potential agglomeration issues upon particle drying. Centrifugation may be considered in this second type of approach. The aim of this technique is to activate the sedimentation of the particles by action of a centrifugal force. This particle settling effect enables then to exchange (generally at the occasion of many successive rounds) most of the supernatant with pure solvent, thus leading progressively to purified suspensions. However, regular centrifugation often shows limitations for the sedimentation of nano-sized particles, while the use of ultracentrifugation can only be dedicated to purify small volumes of suspensions and appears rather energy- and time-consuming.

Based on the above considerations, we have investigated here, from a physico-chemical viewpoint, the purification process of hybrid biomimetic apatite-based colloidal nanoparticles by way of dialysis (in aqueous conditions). Dialysis is indeed another method based on the second type of purification approach, during which the nanoparticles remain in liquid medium at all times. Dialysis is largely used in medicine for example for treating kidney diseases. Unlike ultrafiltration or reverse osmosis, dialysis does not need to apply a gradient pressure, which thus presents an obvious practical advantage, and remains a rather cheap method. It is based on the diffusion of molecules through a permeable membrane due to a concentration gradient [21] which is applied between both sides of the membrane: the dissolved substances (e.g. unreacted ions or un-adsorbed organic molecules) move from the high-concentration region (inside the membrane) to the low-concentration region (outside the membrane). Despite the use of dialysis for specific medical treatments, purification studies of nanoparticle-based systems are very scarce in the literature, and generally remain poorly documented from a physico-chemical viewpoint.

In the present contribution, we studied the dialysis purification of such apatite-based colloidal suspensions intended for biomedical applications, in the case of both Eu-doped and Eu-free systems. We report complementary physico-chemical data on the follow-up of the dialysis efficacy. Particular attention was dedicated to various physico-chemical parameters including conductivity, pH, temperature and the nature of dialysis medium.

2. Materials and methods

2.1. Preparation of apatite-based colloids

The hybrid mineral-organic apatite-based colloids prepared in this work were obtained by coprecipitation at room temperature of calcium and europium nitrates and ammonium hydrogen-phosphate in deionised water, at pH 9.5, in the presence of a biocompatible stabilizing agent: 2-aminoethylphosphate or "AEP", responding to the formula $NH_3^+–CH_2–CH_2–O–P(O)(O^-)_2$. the precipitates were then allowed to age in an oven preset to $100\,°C$ for 16 h. The AEP molecules represent the polar head of a natural phospholipid, phosphatidyl-ethanolamine, that is already present on the lipid bi-layer of human cells [22]. Our previous investigations indicated that such AEP$^-$ molecules could strongly interact with surface calcium ions, thus exerting both an electro-steric repulsive effect preventing/limiting the agglomeration of adjacent nanoparticles, and thus providing colloidal stability to the nanocrystalline apatite suspensions [20,23,24]. Unless otherwise specified, for these colloidal suspensions the starting AEP/(Ca + Eu) molar ratio was set to 1. This value has indeed been shown [20,24] to lead to stable deagglomerated apatite particles with mean particle size around 30 nm.

For each preparation, three aqueous solutions were prepared: solution (A) contained a total of 4.87 mmol of calcium nitrate $(Ca(NO_3)_2 \cdot 4H_2O)$ and europium nitrate $(Eu(NO_3)_3 \cdot 6H_2O)$ with Eu/(Eu + Ca) molar ratio in the initial reaction mixture fixed at 1.5%. Solution (B) contained 4.87 mmol of AEP in deionised water. Finally, solution (C) was prepared from dissolving 1.62 mmol of ammonium hydrogenphosphate in deionised water, with an initial molar ratio (Ca + Eu)/P of 0.33 (ratio used previously for the preparation of apatite colloids in the presence of AEP [20,24]. Solution (A) was mixed with solution (B) under constant stirring. The acidic pH of the resulting solution, leading to solution (D), as well as that of solution (C) were adjusted to 9.5 by addition of ammonia. This alkaline pH was chosen in order to favour the precipitation of apatite rather close to stoichiometry exhibiting good chemical stability [20,24]. The pH of the colloids may be adjusted, after synthesis, to physiological value (7–7.6) in view of biological applications.

For comparative purposes, "reference" non-colloidal apatite suspensions were also synthesized, using a similar protocol as above but without addition of AEP. In this case, solution (B) contained only deionised water.

2.2. Dialysis protocol

In a typical dialysis procedure for this study, a tubular cellulose membrane (length: 15 cm, diameter: 3 cm, cut-off: 6000–8000 Da) was contacted with deionised water during 5 min for preliminary hydration. After clamping the lower end of the membrane, 25 ml of the suspension to dialyse were introduced and the second end was clamped while leaving an open space above the liquid level of about 7 ml filled with air. The membrane was suspended vertically by way of a fixing device and introduced in 800 ml of dialysis medium (e.g. deionised water). As mentioned in the text, the washing medium was continually homogenized by mechanical stirring, and was regularly exchanged by a fresh one (up to 3 days) so as to regenerate the concentration gradient and accelerate the purification process. Unless otherwise specified, the dialysis process was carried out at room temperature ($25\,°C$). Some experiments, as indicated in the text, were run at $45\,°C$. In this case, the response of the conductivity electrode was then corrected for temperature effects based on preliminary calibration.

The principle of dialysis is shown on Fig. 1. During this process the dissolved unreacted species (Ca^{2+}, PO_4^{3-}, AEP$^-$ and co-ions: NO_3^-, NH_4^+) moved by the concentration gradient, cross the pores
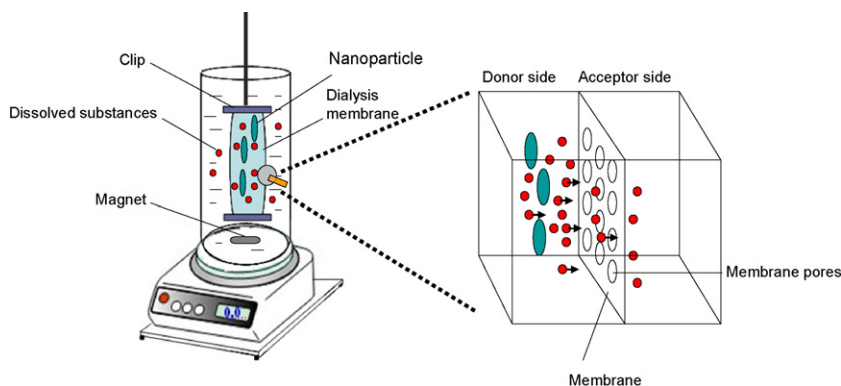
Fig. 1. Schematic principle of the dialysis process.

of the membrane by diffusion, ending up in the dialysis medium (dialysate). The membrane thus behaves like a sieve retaining the solid particles. In this work, the evolution of the dialysis efficacy was followed by conductimetry (platinum electrode) located in the dialysate. In addition, at different stages during dialysis, a part of the apatite suspensions was sampled and freeze-dried in view of physico-chemical powder characterization. The pH of the solution inside and outside the membrane was also followed by use of a pH electrode, during the purification process, with a multi-parameter analyzer (Consort, model C861).

2.3. Physical–chemical characterization

The crystallographic structure of the powders obtained after freeze-drying was investigated by way of X-ray diffraction (XRD) using a CPS 120 INEL diffractometer with the $K_{\alpha 1}$ Cobalt radiation ($\lambda = 1.78892$ Å).

Fourier transform infrared (FTIR) spectroscopy analyses were performed on a Nicolet 5700 spectrometer, in the wavenumber range 400–4000 cm^{-1} (resolution 4 cm^{-1}).

The morphology and size of the nanoparticles were followed by transmission electron microscopy (TEM) on a JOEL JEM-1011 set at 100 keV. For these TEM observations, the suspensions were briefly sonicated (50 KHz, 30 s) and the carbon-coated copper TEM-grids were rapidly dipped into the suspension and allowed to dry prior to analysis.

Rheological measurements (viscosity determinations) were carried out at room temperature on an Anton Paar rheometer, model MCR 301, using a variable shear rate in the range 10–1000 s^{-1}.

Ca and Eu contents were measured by induced coupled plasma atomic emission spectroscopy, ICP-AES (relative uncertainty: 3%). The mineral phosphate content in the samples was determined by colorimetry at $\lambda = 460$ nm using the yellow phospho-vanado-molybdenum acid complex (relative uncertainty: 0.5%). The AEP content in the colloids was evaluated from nitrogen micro-analysis (relative uncertainty: 0.4%).

3. Results and discussion

As a first step, the progression of the purification process by dialysis was investigated in the case of a Eu-free colloid. In this experiment, the dialysis was carried out over a total of 3 days, at room temperature and using deionised water as dialysis medium. In view of regenerating the concentration gradient in the washing medium, the latter was changed every 4 h (except at night where it was left during 16 h). The evolution of the dialysis process was followed by FTIR spectroscopy analysis on the freeze-dried suspensions remaining inside the membrane after increasing periods of

dialysis time (Fig. 2a). Note that this spectroscopy technique was preferred over other techniques (e.g. XRD) as a probe for purity, due to its greater level of resolution for detecting the presence of many types of trace impurities.

At time zero (non-dialysed sample), the FTIR spectrum exhibited wide absorption bands, especially at 3176, 1000 and 500 cm^{-1} due to the presence of large amounts of unreacted species. Although the FTIR spectrum of apatite was not easily identifiable due to band overlapping, the bands observed around 1024 and 601 cm^{-1} are respectively characteristic of PO$_4$$^{3-}$ ν_3 and ν_4 vibration modes in apatite. Besides, the observation of the thin peak at 1383 cm^{-1} characteristic of nitrate ions appears as one parameter for monitoring the purification state of the colloidal suspension upon dialysis, at least for high nitrate concentrations. Indeed, this nitrate absorption band falls in the same absorption region as carbonate ions which
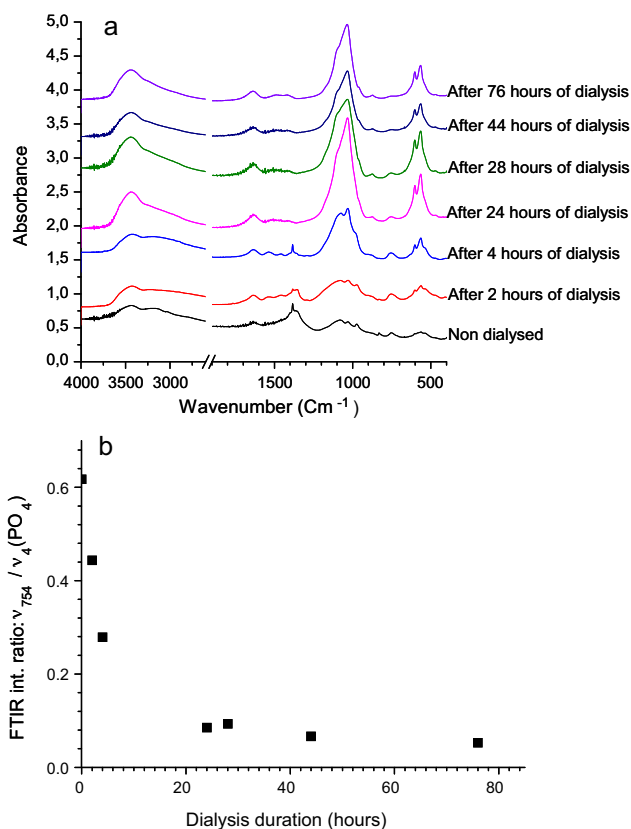

Fig. 2. Evolution of (a) FTIR spectra vs. dialysis time for Eu-free apatite colloid and (b) FTIR intensity ratio ν_{754}/ν_3(PO$_4$).

often appear as trace impurities in apatite-based compounds and do not enable nitrate evaluations for low concentrations. Finally, another absorption band can be observed around 754 cm^{-1}, which is assignable to AEP molecules in the system (as already commented in a previous work [24]).

After 2 h of dialysis, the FTIR spectrum shows that the intensity of the nitrate peak has started to decrease, witnessing the migration of such unreacted species from the donor side to the acceptor side of the membrane (see Fig. 1). This is also confirmed by a better detection of the peaks of PO$_4$$^{3-}$ and AEP. Nevertheless the characteristic apatite IR spectrum still remains only partially visible at this stage. In contrast, after 4 h of dialysis the apatite IR profile becomes clearly identifiable, revealing that an important part of unreacted species has been transferred to the dialysis medium, outside the membrane. However, the presence of nitrate ions is still noticed at 1383 cm^{-1}.

FTIR data indicate that the purification process of the colloidal suspension was achieved after ca. 24 h of dialysis, as pointed out in Fig. 2a. Indeed, at t = 24 h, no remaining traces of unreacted salts can be detected by FTIR, and all the characteristic absorption bands of apatite are observed, particularly around 1095, 1024, 601 and 563 cm^{-1} (assigned to the PO$_4$$^{3-}$ ν_3 and ν_4 vibration modes). The peak observed at 875 cm^{-1} is, for its part, due to HPO$_4$$^{2-}$ ions from the apatite particle [25].

The follow-up of the intensity of the AEP-related band at 754 cm^{-1} is another way to evaluate the efficacy of the dialysis process. Indeed, it enables to monitor the total amount of AEP in the system, including unreacted AEP molecules. Fig. 2b shows the evolution of the ratio between the integrated intensities of the AEP-related band at 754 cm^{-1} and the (multiple) band that exhibits a maximum absorption at 565 cm^{-1} (corresponding to ν_4(PO$_4$) from apatite phosphate groups). The curve obtained versus time points out a significant decrease of the amount of AEP in the medium, especially during the first 4 h of dialysis. In contrast, the AEP content in the suspensions after ca. 10 h of dialysis was found to stabilize. This stabilization then points out the complete elimination of unreacted AEP$^-$ molecular ions at this stage. The only remaining AEP molecules are those grafted on the apatite colloidal nanoparticles. Chemical analyses on the dialysed nanoparticles led at this point to the molar ratio AEP/apatite of 0.81 (with a nonstoichiometric apatite phase exhibiting a Ca/P ratio close to 1.4).

It can be noted that a progressive increase of the suspension viscosity was also observed for extended periods of dialysis (noticeable beyond 5 h). However, the quantification of the viscosity of such suspensions was found to be rather complex as we observed their non-Newtonian character, exhibiting a shear-thinning behaviour with the apparent viscosity depending on the shear rate applied. Generally speaking, the initial apparent viscosity of the starting suspensions was found in the range 1–2 mPa s for shear rates of 100–1000 s^{-1}, while it gained more than one order of magnitude after dialysis. We showed earlier [24] that the presence of AEP during apatite precipitation efficiently limited nanocrystals agglomeration (by way of electro-steric hindrance between adjacent nanoparticles) thus enabling to obtain stable colloids. In this context, an increase in the suspension viscosity may be linked to the desorption of some AEP molecules, allowing then some inter-particle bridging. This may indeed be particularly possible in the case of such ionic crystals (apatite) where dissolution–reprecipitation phenomena may arise rather easily (where reprecipitation may then possibly be undergone with fewer AEP molecules than initially). Although the above results indicated that the dialysis process still remained efficient despite a rise in viscosity, it was interesting to investigate potential ways to limit this viscosity increase. An experiment was carried out by performing the dialysis purification in deionised water enriched with AEP in order to lower specifically the AEP concentration gradient between
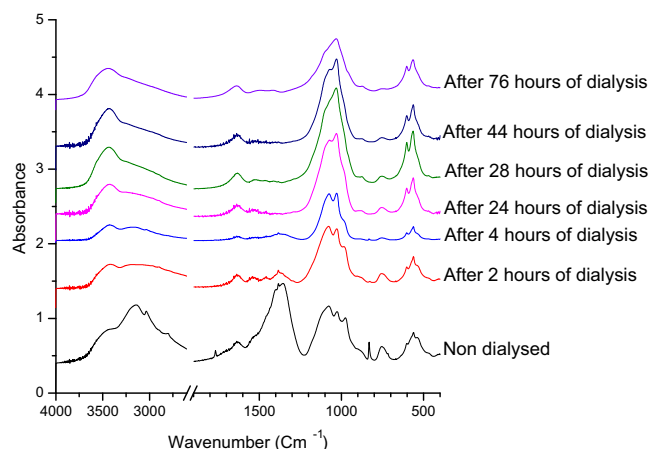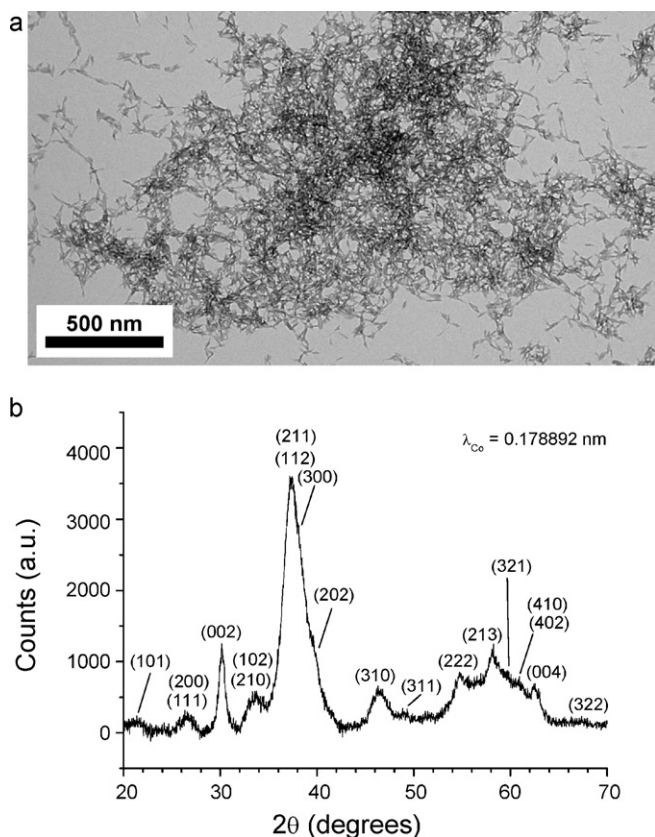

Fig. 3. Evolution of FTIR spectra vs. dialysis time for apatite colloid doped with 1.5 mol.% Eu (relative to Ca).

both sides of the membrane and therefore potentially limit AEP desorption. In this case, FTIR analysis of the freeze-dried suspension shows indeed a greater remaining amount of AEP, confirming the slower migration of these molecules through the membrane. However, no significant decrease in the viscosity of the dialysed suspension was noticed. Another possible cause for modifications in the AEP/apatite surface interaction can be the pH decrease undergone during dialysis. A dialysis experiment was then run in water enriched with sodium hydroxide up to pH 9. However, again, no major change was observed on the final suspension viscosity. Taking into account these findings, it is probable that the viscosity increase may be linked to the departure (upon dialysis) of all unreacted ionic species including the "counter-ions" located around each AEP-covered nanoparticle that may help hindering the formation of interactions between adjacent particles. It should indeed be noted that the ammonium –NH$_3$$^+$ groups from the AEP molecules confer an overall positive surface charge to the colloidal nanoparticles (while the phosphate end of AEP interacts with the apatite surface) as reported elsewhere [20]. However, since no sedimentation is detected throughout the dialysis process, this newly created array of interactions among nanoparticles is probably rather weak and does not lead to destabilization of the colloid nor to the hindrance of the purification process.

All the above-mentioned considerations on the dialysis of Eu-free apatite colloids were also found to apply to suspensions doped with europium (Fig. 3). The europium content used in this work was 2 ± 0.2 mol.% relative to calcium, as measured by ICP-AES, and was obtained by using an initial molar ratio Eu/(Eu + Ca) in the precipitating medium of 1.5%. It can however be noticed that the purification process for this Eu-doped colloid seemed to be completely achieved after 28 h rather than 24 h for the Eu-free suspension. In a previous work [20] we showed that the incorporation of Eu^{3+} ions in the composition of such apatites led to some modifications of physico-chemical features, including in terms of crystallinity state or stoichiometry, and this was assigned to an inhibitory effect of Eu on apatite crystal growth. The slight differences observed on dialysis behaviours are thus also likely to be linked to intrinsic variations in the characteristics of non-doped and Eu-doped apatite colloids.
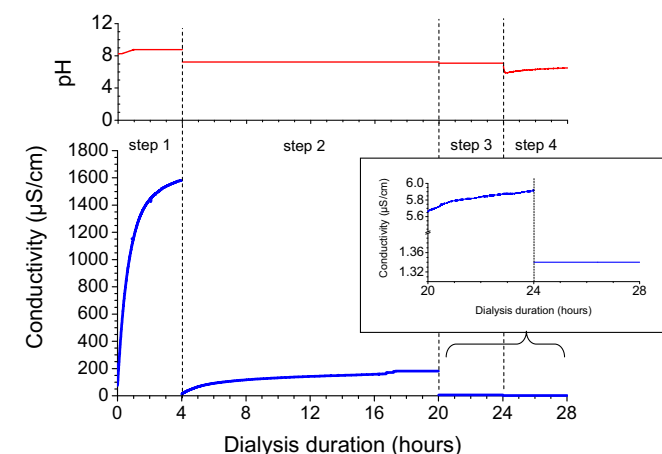
The efficiency of dialysis was also demonstrated by transmission electron microscopy (TEM) observations (Fig. 4a) which were performed on the colloidal suspensions doped with 2% Eu (relative to Ca) dialysed for 24 h. The micrograph shows indeed that the apatite nanoparticles are well dispersed and homogenous in shape, pointing out the removal of unreacted species. Also, we can note that the particles dimensions are around 28 nm in length and 9 nm in width,

Fig. 4. (a) TEM micrograph for Eu-doped apatite colloid (2% Eu relative to Ca) dialysed for 24 h in deionised water and (b) related XRD pattern with apatite peak indexation.

enabling then to envision their use in the biomedical domain for example for intracellular applications requiring typically nanoparticles smaller than 100 nm. The XRD pattern of this dialysed sample was also recorded for cross-check (Fig. 4b) confirming the apatitic nature of the sample with no detectable impurity.

The evolution of the pH of the dialysis medium was followed as a function of time (Fig. 5). The dialysis was performed here at room temperature and in the form of 4 successive steps, and the dialysis medium (deionised water, initial pH close to 6.5) was changed before each step for regenerating concentration gradients. After initiation of the dialysis process, the pH of the dialysate was found to

Fig. 5. Evolution of the conductivity and pH of the dialysis medium vs. time for apatite colloid doped with 1.5 mol.% Eu (relative to Ca).

increase within few minutes to about 8.5 and remained rather stable for the whole duration of step 1 (first 4 h of dialysis), witnessing the fast diffusion of OH− ions through the membrane. During steps 2 and 3, lasting respectively 16 (overnight) and 4 h, the pH value was globally constant in the range 7.1–7.25 and it reached 6.5 during step 4. This overall pH evolution versus dialysis time depicts the progressive elimination of hydroxide ions from the dialysing suspension and illustrates the efficacy of dialysis, which is confirmed by the final slightly acidic/neutral pH values observed in the dialysing medium.

The dialysis process was also followed by conductimetry in Fig. 5, by monitoring the conductivity of the dialysis medium (outside the membrane) versus time. During the first 4 h of dialysis (step 1) the conductivity in the dialysis medium increased rapidly from 75 to 1581 $\mu S\,cm^{-1}$. The initial value of 75 $\mu S\,cm^{-1}$ (obtained 5 s after starting the dialysis process) is greater than the typical value of deionised water (1.3–1.5 $\mu S\,cm^{-1}$) and therefore indicates that the purification process starts as soon as the membrane is introduced into the dialysis medium. This can be explained by the occurrence of strong concentration gradients at this stage. Around the fourth hour of dialysis, the conductivity started to stabilize and the medium was then changed by a fresh one in order to regenerate the concentration gradients. In the second step of dialysis (step 2, lasting 16 h), the conductivity value increased from 12.24 to 159.6 $\mu S\,cm^{-1}$. It can be noted that after the first 4 h of step 2 the conductivity value only reached 117 $\mu S\,cm^{-1}$ as compared to 1581 $\mu S\,cm^{-1}$ at the end of step 1. This low level of conductivity is indicative of small concentrations of remaining unreacted species. At the end of step 2 the conductivity barely reached only 159 $\mu S\,cm^{-1}$ and led to a constant level. Although the FTIR data reported on Figs. 2 and 3 pointed out the continuing progression of the purification/dialysis efficacy even beyond 20 h, the conductivity monitored during steps 3 and 4 from Fig. 5 was extremely low, thus indicating a noticeable level of purification. The high sensitivity of the FTIR spectroscopy technique can then be used to refine the final steps of purification.

Each step of the conductivity curve, until complete stabilization, can be described by a rapid rise of the conductivity followed by a progressive stabilization. This evolution with time does not fit to a simple logarithmic law and is better graphically described in a first approximation by an equation of the type: $y = a - b\exp(-kt)$. It is important to keep in mind at this point that the conductivity of a solution/electrolyte is directly linked to the concentration of each ion constituting the solution, by way of a linear combination involving also the ions charge and size/weight. Therefore, the increase in conductivity is directly related to the increase in the ionic concentration of the ions passing into the dialysis medium.

Mathematical modelling of membrane permeation has been studied in the literature [26,27] based in particular on Fick's diffusion laws. At a given temperature and in the case of a single solute contained in a solution of volume V and in contact with the surface S of a membrane, the concentration of solute inside the membrane at time t, noted "$c_{int}(t)$", is show [26,27] to follow the equation:

$$\ln\left(\frac{c_{int}(t)}{c_0}\right) = -\frac{SP}{V}t \tag{1}$$

or equivalently:

$$c_{int}(t) = c_0\exp\left(-\frac{SP}{V}t\right) \tag{2}$$

where c_0 is the initial concentration of the solute in the solution and P is the membrane permeability relative to this solute; with P depending on the nature and characteristics of the membrane and of the solute as well as on the temperature. Taking into account the mass balance for the solute, stating that the total number of moles of solute is distributed inside and outside the membrane, the solute

concentration "$c_{ext}(t)$" in the dialysis medium of volume V_{ext} is then given by:

$$c_{ext}(t) = c_0 \frac{V}{V_{ext}} \left[1 - \exp\left(-\frac{SP}{V} t \right) \right] = a \left[1 - \exp\left(-\frac{SP}{V} t \right) \right] \quad (3)$$

where the parameter "a" thus depends on the initial concentration in the solute.

If several solutes are present in the solution, each solute concentration in the dialysate will thus theoretically follow an equation of the form of Eq. (3), at least if interactions between dialyzing ions may be neglected. Since the conductivity of the dialysate (which was experimentally measured here) is a linear combination of the concentrations of the "n" ions present in the system, the overall conductivity $C_{sol}(t)$ varies thus as:

$$C_{sol}(t) = a_0 + \sum_n \lambda_n a_n \left[1 - \exp\left(-\frac{SP_n}{V} t \right) \right] \quad (4)$$

where "a_0" is the initial conductivity of the dialysis medium, "a_n" and "P_n" are the parameters equivalent to "a" and "P" in Eq. (3), and "λ_n" is the molar conductivity of the ion "n" (depending on the size and charge of the ion).

Various types of diffusing ions, either mineral (calcium, europium, phosphate, nitrate, ammonium and hydroxide) or organic (AEP$^-$) are involved in the present study. Since these ions differ by their ionic charges and sizes, they are likely to lead to different diffusion kinetics/membrane permeabilities, and it was not possible here to separate the contribution of each ionic species. However, it is interesting to remark that the conductivity profiles obtained are, as could be expected, in perfect agreement with the mathematical expression of Eq. (4) which can explain the overall "$a - b \exp(-kt)$" type of variation.

The first 4 h of dialysis were also followed, at room temperature, in the case of starting suspensions prepared in the presence of decreasing amounts of AEP in the precipitating mixture. The ratios investigated were AEP/(Ca + Eu) = 0.4, 0.6 and 0.8, while the above-mentioned data were obtained with AEP/(Ca + Eu) = 1. These three additional values were also shown in a previous work [20] to lead to stable apatite colloids, and we demonstrated that it was possible to tailor the mean nanoparticle size in the range 30–100 nm by controlling the amount of AEP in the precipitating medium. It was thus interesting to check here how the conductivity profile of the dialysis medium would be impacted by a change in the total AEP content in the suspension. Our measures showed that the conductivity increased rather monotonously with the AEP/(Ca + Eu) ratio in the starting suspension, ranging from 1079 to 1633 μS cm^{-1} after 4 h of dialysis. The fact that the conductivity curve follows straightforwardly the relative amount of AEP is another direct evidence that the diffusion of the AEP$^-$ molecular ions through the dialysis membrane starts as soon as the dialysis process is initiated. Thus, the diffusion of AEP through the dialysis membrane does not seem to be particularly limited despite a size slightly higher than the size of the mineral ions present in the system. Also, since a change in the starting AEP content in the system allows to prepare apatite colloids with tailorable nanoparticle sizes, so as to adapt their characteristics to specific biomedical applications, it is interesting to point out that the dialysis process as described in the present work can apply for any of such apatite-based colloids, independently of the AEP content.

The conductivity profile corresponding to the first 4 h of dialysis carried out in deionised water at 25 °C (step 1 from Fig. 5) was replotted in Fig. 6 and compared to the equivalent curve obtained at 45 °C. Profile analysis showed that, again in this latter case, a multiple exponential-based equation corresponding to Eq. (4) could be applied to fit the conductivity plot. Nonetheless, the stabilized level of conductivity reached after 4 h at 45 °C (1879 μS cm^{-1}) was found to be noticeably higher than the corresponding value
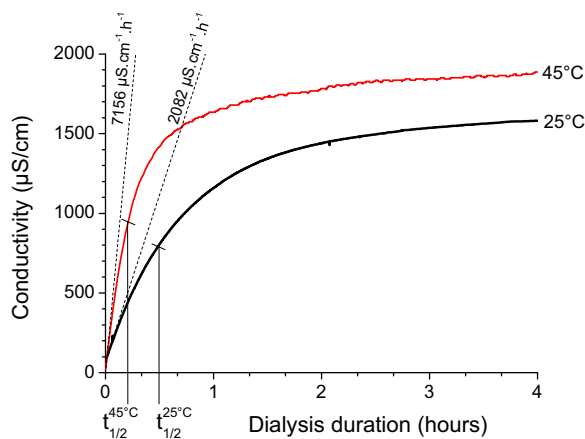
Fig. 6. Effect of dialysis temperature (25 and 45 °C) on conductivity in the dialysis medium, with slopes at origin and half-times of dialysis.

(1581 μS cm^{-1}) measured at 25 °C. Moreover the half-time of dialysis "$t_{1/2}$", corresponding to the time for which half of the stabilized level of conductivity is reached, was found to be 0.21 h at 45 °C as compared to 0.48 h at 25 °C. These findings point out the greater amount of diffusing ions and faster kinetics of diffusion when the dialysis process was performed at higher temperature. This increase in dialysis rate can also be visualized by comparing the slopes at the origin of the conductivity curves (materialized by dotted lines in Fig. 6), namely 2082 and 7156 μS cm^{-1} h^{-1} respectively for 25 and 45 °C, unveiling a ratio of ca. 3.4 between the two values. This temperature acceleration effect can be related to an increased thermal activation of the dialyzing ions, enabling these species to cross more rapidly the dialysis membrane in view of equalizing their chemical potentials (and therefore minimizing concentration gradients). The possibility to activate such purification processes by increasing the dialysis temperature could then be seen as an interesting way to reduce further dialysis durations, for example in view of industrial scale-up.

Another potential way to activate dialysis processes may be to shorten the length of each dialysis step, thus leading to a more frequent change of washing medium. In an additional experiment, dialysis was carried out using a frequency of 1 h for the change in dialysis media, with a total of 3 consecutive steps. FTIR spectroscopy analysis indicated however in this case a spectrum highly similar to the one obtained previously after 4 consecutive hours without interruption. These findings indicate that the gain in dialysis efficacy related to this protocol did not enable to shorten noticeably the overall dialysis length, and this method does not seem to be interesting to retain.

4. Concluding remarks

The purification by dialysis of colloids based on biomimetic nanocrystalline apatites, either doped or non-doped with europium ions, was investigated in detail in this work by way of several complementary techniques including in particular FTIR, TEM, XRD, conductivity and pH measurements. The effect of a change in temperature, dialysis medium, and in the starting colloid formulation (varying AEP contents) were also followed and discussed. Mathematical modelling was applied and commented to explain the observed conductivity data.

In this work, we pointed out the possibility to carry out rather easily some punctual purity evaluations throughout the dialysis process so as to adapt it to the system to dialyse, thanks to fast techniques such as FTIR and conductivity measurements. Besides, we showed that the dialysis process was a well-adapted cheap tech-

nique to purify such mineral–organic hybrid colloidal suspensions intended for biomedical applications, where the elimination of all unreacted species is a crucial step in view of pass/no-pass check towards future clinical developments.

References

[1] Y. Lu, P.S. Low, Adv. Drug Deliv. Rev. 54 (2002) 675.
[2] D. Pan, J.L. Turner, K.L. Wooly, Chem. Commun. 19 (2003) 2400.
[3] X. Montet, K. Montet-Abou, F. Reynolds, R. Weissleder, L. Josephson, Neoplasia 8 (2006) 214.
[4] P. Chan, M. Kurisawa, J.E. Chung, Y. Yang, Biomaterials 28 (2007) 540.
[5] S. Soppimath, L.H. Liu, W.Y. Seow, S.Q. Liu, R. Powell, P. Chan, Y.Y. Yang, Adv. Funct. Mater. 17 (2007) 355.
[6] United Nations Department of Economic and Social Affairs, World Population Prospects: The 2006 Revision, United Nations, New York, 2007.
[7] A. Miyawaki, Dev. Cell 4 (2003) 295.
[8] M. Bruchez, M. Moronne, P. Gin, S. Weiss, A.P. Alivisatos, Science 281 (1998) 2013.
[9] W.J. Parak, D. Gerion, T. Pellegrino, D. Zanchet, C. Micheel, S.C. Williams, R. Boudreau, M.A. Le Gros, C.A. Larabel, A.P. Alivisatos, Nanotechnology 14 (2003) R15.
[10] F. Meiser, C. Cortez, F. Caruso, Angew. Chem. 43 (2004) 5954.
[11] B. Ballou, B.C. Lagerholm, L.A. Ernst, M.P. Bruchez, A.S. Waggoner, Bioconjug. Chem. 15 (2004) 79.
[12] A.M. Derfus, W.C.W. Chan, S.N. Bhatia, Nano Lett. 4 (2004) 11.
[13] K.T. Shimizu, R.G. Neuhauser, C.A. Leatherdale, S.A. Empedocles, W.K. Woo, M.G. Bawendi, Phys. Rev. B 63 (2001) 205.
[14] X. Brokmann, J.P. Hermier, G. Messin, P. Desbiolles, J.P. Bouchaud, M. Dahan, Phys. Rev. Lett. 90 (2003) 120601.1.
[15] H. Meyssamy, K. Riwotzki, A. Kornowski, S. Naused, M. Haase, Adv. Mater. 11 (1999) 840.
[16] K. Riwotzki, H. Meyssamy, A. Kornowski, M. Haase, J. Phys. Chem. 104 (2000) 2824.
[17] K. Riwotzki, H. Meyssamy, H. Schnablegger, A. Kornowski, M. Haase, Angew. Chem. 40 (2001) 573.
[18] P. Schuetz, F. Caruso, Chem. Mater. 14 (2002) 4509.
[19] R.Z. Legeros, in: B. Pamplin (Ed.), Progress in Crystal Growth And Characterization Of Materials, vol. 4, Pergamon Press, New York, 1981, pp. 1–45.
[20] A. Al-kattan, P. Dufour, J. Dexpert-Ghys, C. Drouet, J. Phys. Chem. C 114 (2010) 2918.
[21] J. Pastor, A.M. Pauli, Techniques de l'ingénieur – Analyse et Caractérisation P2 (1995) 1525.1.
[22] L. Rothfield, A. Finkelstein, Annu. Rev. Biochem. 37 (1968) 463.
[23] J.Y. Chane-Ching, A. Lebugle, I. Rousselot, A. Pourpoint, F. Pellé, J. Mater. Chem. 17 (2007) 2904.
[24] A. Bouladjine, A. Al-kattan, P. Dufour, C. Drouet, Langmuir 25 (2009) 12656.
[25] C. Rey, C. Combes, C. Drouet, A. Lebugle, H. Sfihi, A. Barroug, Materialwiss. Werkstofftech. 38 (2007) 1.
[26] D.F. Shieh, J. Feijen, D.J. Lyman, Anal. Chem. 47 (1975) 1186.
[27] M.C. Annesini, A. Memoli, S. Petralito, J. Membr. Sci. 180 (2000) 121.